Core-Orthogonalization Pattern on the Contour Map of Positron Annihilation A(γ)-Function

Bull. Coll. Med. Sci. Tohoku Univ. 6(2) : 89～96, 1997

Core-Orthogonalization Pattern on the Contour Map of Positron Annihilation $A(r)$-Function

Teiji KOBAYASI

General Education, College of Medical Sciences, Tohoku University

ポジトロン消滅 $A(r)$-関数マップ上の内殻電子直交化パターン

小林悌二

東北大学医療技術短期大学部 総合教育

Key words: Positron annihilation, $A(r)$-function, Core-orthogonalization effect, Pseudopotential theory, Semiconductor

In the pseudopotential calculation of the valence electron-positron $A(r)$-function of the valence electron system of semiconducting material Ge, the quantum-mechanical orthogonalization between the valence and the inner core electronic states has been taken into account. The function is the Fourier inversion transform of the momentum density distribution of the electron-positron pairs. A characteristic local pattern is observed near the atomic position on the contour map of the $A(r)$-function.

In relation to an analogous pattern on the corresponding Compton $B(r)$-function reflecting well the position and the size of one of the intra-unit-cell atoms, it has been discussed that the local pattern represents a kind of atom image modified by the characteristic distribution of positron in crystal.

The pseudopotential (PP) theory including the core-orthogonalization (CO) is a powerful tool for detailed investigation of valence electron distributions in real and momentum spaces in semiconducting materials[1)~8)]. In the PP theory, the wave function of valence electron is composed of two parts. The main part is a pseudo-wave function which describes a relatively smooth-varying behaviour of the electron in the crystal. The second part describes a spatially rapid oscillation of the electron in the vicinity of inner core region of atoms. The local oscillation comes from the fact that the valence electronic states should be quantum-mechanically orthogonal to the core electronic states. The *true* valence electron wave function can be obtained by orthogonalizing the pseudo-wave function mathematically to all of the core electron wave functions. As discussed in detail in refs. 1-8, the local oscillation due to the CO terms in the wave function introduces many interesting effects into the electron charge and momentum distributions, the Compton profiles, the electron-positron momentum distribution and the angular correlation of annihilation radiation in the valence electron

system.

In a previous paper[8] discussing CO effects on Compton scattering in crystalline Si and Ge, it was shown that an atom-like pattern appears on the contour map of the Compton $B(\boldsymbol{r})$-function, as if the Compton scattering works as a microscope to detect a local structure of the crystal via the CO terms. Here, the function $B(\boldsymbol{r})$ is the Fourier inversion transform of the momentum density distribution[3)9)~15)] of valence electrons. The pattern corresponds well, in its position and size, to the intra-unit-cell atom in the diamond structure of these materials. This effect is due to the atomic electron-like behaviour of the valence electron near the atomic cores.

The purpose of this paper is to discuss a CO effect on the $A(\boldsymbol{r})$-function in valence electron-positron pair annihilation. The $A(\boldsymbol{r})$-function was introduced[3] by the author as a function corresponding to the $B(\boldsymbol{r})$-function in Compton scattering. It is defined as the Fourier inversion transform of the momentum density distribution of the annihilating *electron-positron pairs* ;

$$A(\boldsymbol{r})=\sum_{\boldsymbol{q}}\Gamma(\boldsymbol{q})\exp(i\boldsymbol{q}\cdot\boldsymbol{r})/\Omega, \qquad (1)$$

where $\Gamma(\boldsymbol{q})$ is the momentum density distribution function of the electron-positron pair momentum $\boldsymbol{q}$ and Ω is the crystal volume. The $\Gamma(\boldsymbol{q})$ is given by

$$\Gamma(\boldsymbol{q})=2\sum_{n}\sum_{k}\left|\int\Psi_{nk}(\boldsymbol{r})\Psi_{+}(\boldsymbol{r})\exp(-i\boldsymbol{q}\cdot\boldsymbol{r})d^3\boldsymbol{r}\right|^2. \qquad (2)$$

Here, Ψ_{nk} is the wave function of the valence electron with wave vector $\boldsymbol{k}$ in the n-th occupied band and Ψ_{+} is the wave function of a *thermalized* positron annihilating with the electron. The $\Gamma(\boldsymbol{q})$ is obtained by replacing the electron wave function Ψ_{nk} in the electron momentum density $\rho(\boldsymbol{q})$ by the electron-positron pair wave function $\Psi_{nk}\Psi_{+}$. Details of the PP energy band calculation for these wave functions and the orthogonalization procedure for Ψ_{nk} are given elsewhere[3)4)16)17)]. Numerical calculation of the CO effect is performed for Ge with many core electronic states originated from the atomic $1s$, $2s$, $2p$, $3s$, $3p$ and $3d$ states.

Contribution of the CO terms to $A(\boldsymbol{r})$ is defined by

$$\Delta A(\boldsymbol{r})=A(\boldsymbol{r})-A^{\text{pseudo}}(\boldsymbol{r}), \qquad (3)$$

where $A^{\text{pseudo}}(\boldsymbol{r})$ is the $A(\boldsymbol{r})$-function in the pseudo valence electron system with no CO consideration. We employ the method of the cubic harmonics expansion[4)13)18)]. For example, $A(\boldsymbol{r})$ is expanded, with radial expansion coefficients $A_{li}(r)$, as

$$A(\boldsymbol{r})=\sum_{l}\sum_{i}A_{li}(r)K_l^i(\Omega_r), \qquad (4)$$

where K_l^i is the l (angular momentum)-th order cubic harmonics belonging to the Γ_1-representation of the O_h group symmetry and i distinguishes the different independent harmonics with the same l. A full convergence of the expansion was attained by inclusion of $l\leq 22$, in which the first sixteen harmonics are contained. The term of $l=0$ corresponds to the spherically symmetric part and the terms of nonzero l describe the anisotropic behaviour of $A(\boldsymbol{r})$ in the positional space of $\boldsymbol{r}$.

Calculations in three dimensional zone of $\boldsymbol{r}$ are performed on the $(1\bar{1}0)$ plane including the five directions of high crystallographic symmetry of [001], [112], [111], [221] and [110]. The Ge-Ge valence bond axis is along the direction [111] with the bonding centre at $\boldsymbol{r}=(1,1,1)a/8$, where a is the lattice constant (Ge : $a=10.6772$ a.u.). Figures 1 and 2 show the contour maps of $A(\boldsymbol{r})$ and $A^{\text{pseudo}}(\boldsymbol{r})$, respectively. In Fig. 1, (a) shows the behaviour of total $A(\boldsymbol{r})$

including very large spherical part and (b) shows the anisotropic part with subtraction of the spherical component from (a). The distance parameter r is in units of a. In Fig. 1(a), the heavy contour line shows zero and the light one is for positive value. The contour spacing is 0.1 in units of $1/\Omega_a$, where the atomic volume Ω_a is a half of the primitive unit cell volume $\Omega_0 = a^3/4$ in the diamond structure. In Fig. 1(b), the heavy, middle and light contour lines show positive, zero and negative values, respectively, and the spacing is 0.005. Directional variations of total $A(\boldsymbol{r})$ along these directions are given in Fig. 2 in ref. 4. In Fig. 2, (a) shows the total

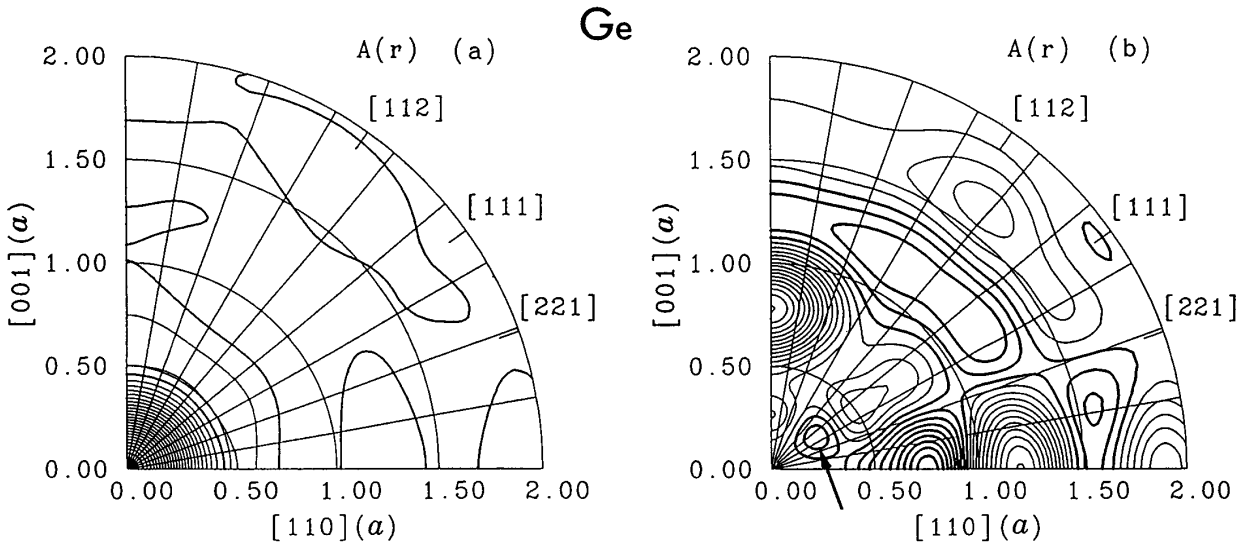

Fig. 1. Contour map of the *true* valence electron $A(\boldsymbol{r})$ of Ge on the $(1\bar{1}0)$ plane: (a) Total $A(\boldsymbol{r})$ including the spherical component. (b) Anisotropic part of $A(\boldsymbol{r})$. Types of contour lines and contour spacing are indicated in the text.

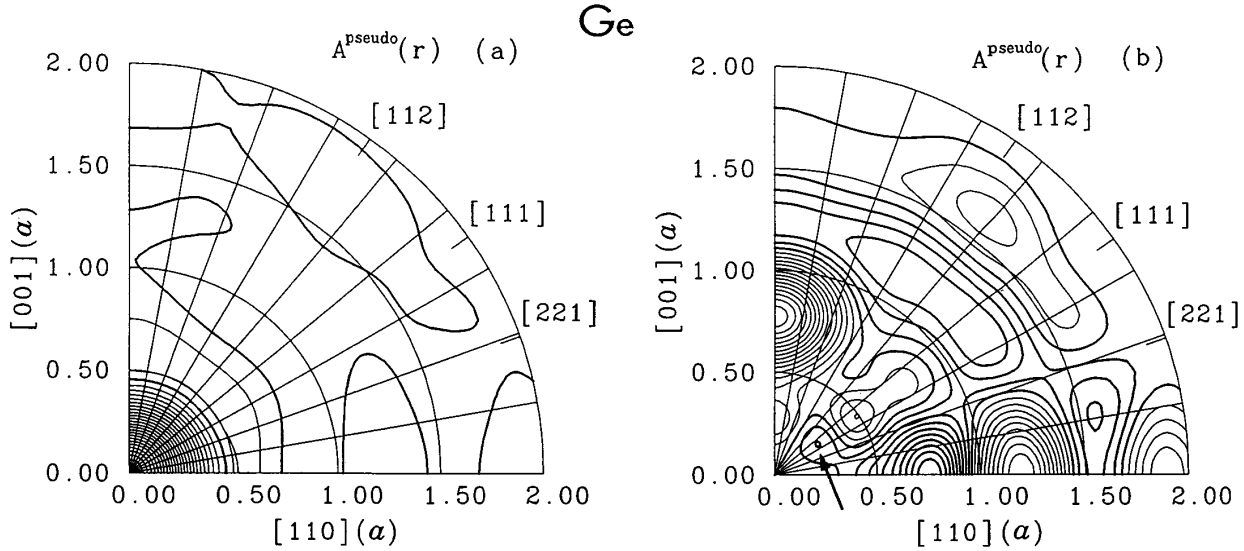

Fig. 2. Contour map of the pseudo valence electron $A^{\text{pseudo}}(\boldsymbol{r})$ of Ge on the $(1\bar{1}0)$ plane: (a) Total $A^{\text{pseudo}}(\boldsymbol{r})$ including the spherical component. (b) Anisotropic part of $A^{\text{pseudo}}(\boldsymbol{r})$. Types of contour lines and contour spacing are indicated in the text.

$A^{\text{pseudo}}(\boldsymbol{r})$ and (b) shows its anisotropic part, in the same contour spacing as in Fig. 1. As can be seen from Figs. 1 and 2, $A(\boldsymbol{r})$ and $A^{\text{pseudo}}(\boldsymbol{r})$ are fundamentally similar to each other, suggesting a small contribution of the CO terms. As arrowed in the anisotropic part of $A^{\text{pseudo}}(\boldsymbol{r})$ [Fig. 2(b)], a local pattern is observed around the point at $r=0.26a$ along the valence bond axis and it remains in the total $A(\boldsymbol{r})$ [Fig. 1(b)]. The centre of the pattern does not coincide with the valence bonding centre at $r=\sqrt{3}a/8=0.2165a$ nor with the nearest neighbour atom

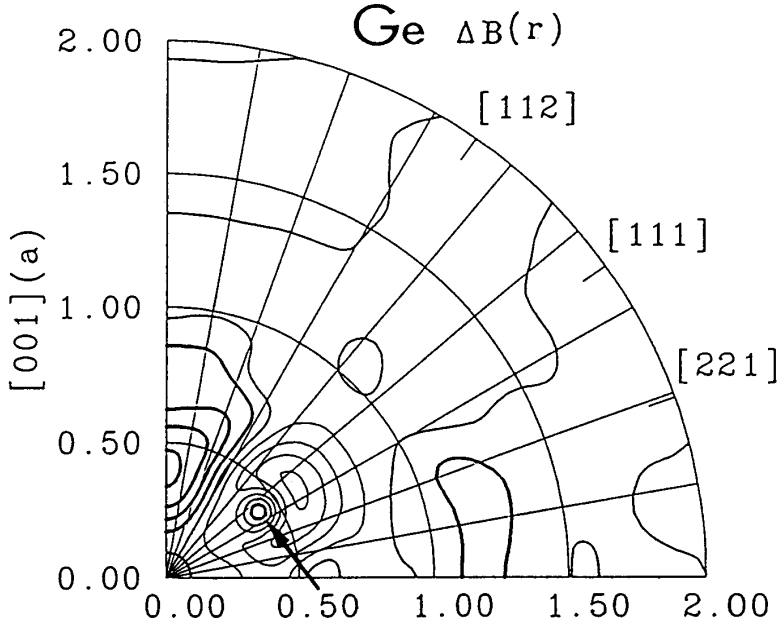

Fig. 3. Contour map of the anisotropic part of Compton $B^{\text{pseudo}}(\boldsymbol{r})$ of Ge on the $(1\bar{1}0)$ plane.

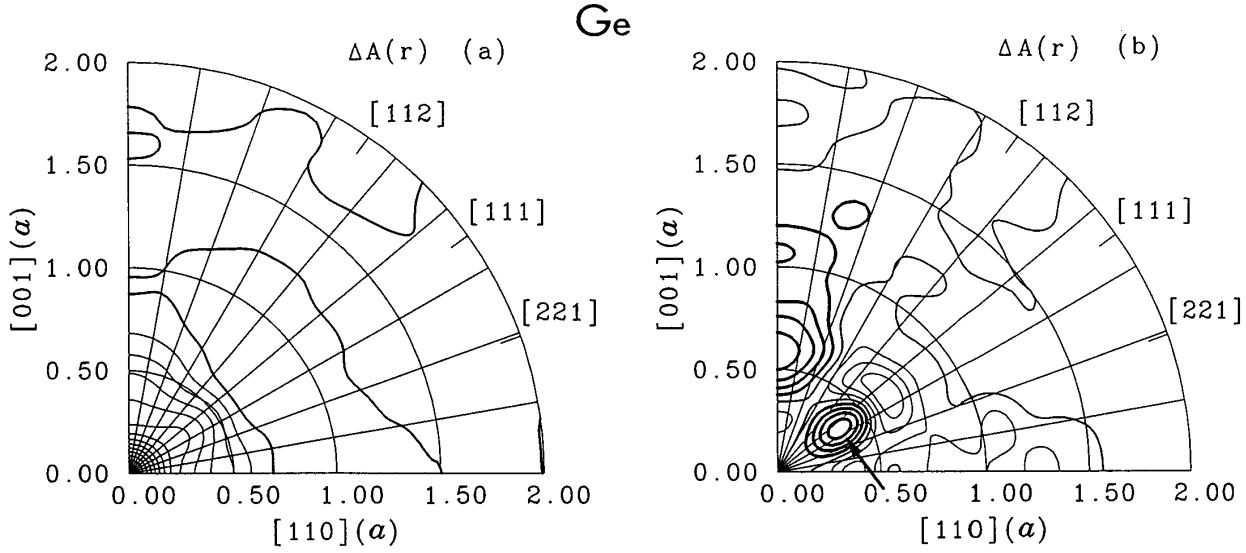

Fig. 4. Contour map of the CO contribution to $A(\boldsymbol{r})$, $\Delta A(\boldsymbol{r})$, of Ge on the $(1\bar{1}0)$ plane: (a) Total $\Delta A(\boldsymbol{r})$ including the spherical component. (b) Anisotropic part of $\Delta A(\boldsymbol{r})$. Types of contour lines and contour spacing are indicated in the text.

site (one of the two sites in the primitive unit cell) at $r=\sqrt{3}a/4=0.4330a$ in the [111] direction.

General feature in contours of $A^{\text{pseudo}}(\boldsymbol{r})$ [Fig. 2(b)] is very similar to that of the Compton $B^{\text{pseudo}}(\boldsymbol{r})$, which is shown in Fig. 3 for comparison, except that such a local pattern mentioned above is not observed in $B^{\text{pseudo}}(\boldsymbol{r})$. Therefore, the local pattern can be connected with the following characteristic distribution of a positron injected into the crystal. As shown in Fig. 4 in ref. 2, during a very short thermalization-time, the positron tends to be strongly repelled away from the atomic core region of repulsive Coulomb potential. It makes a high density peak around the so-called interstitial site with no atoms, where the valence electron density is most vacant (see Figs. 2 and 3 in ref.

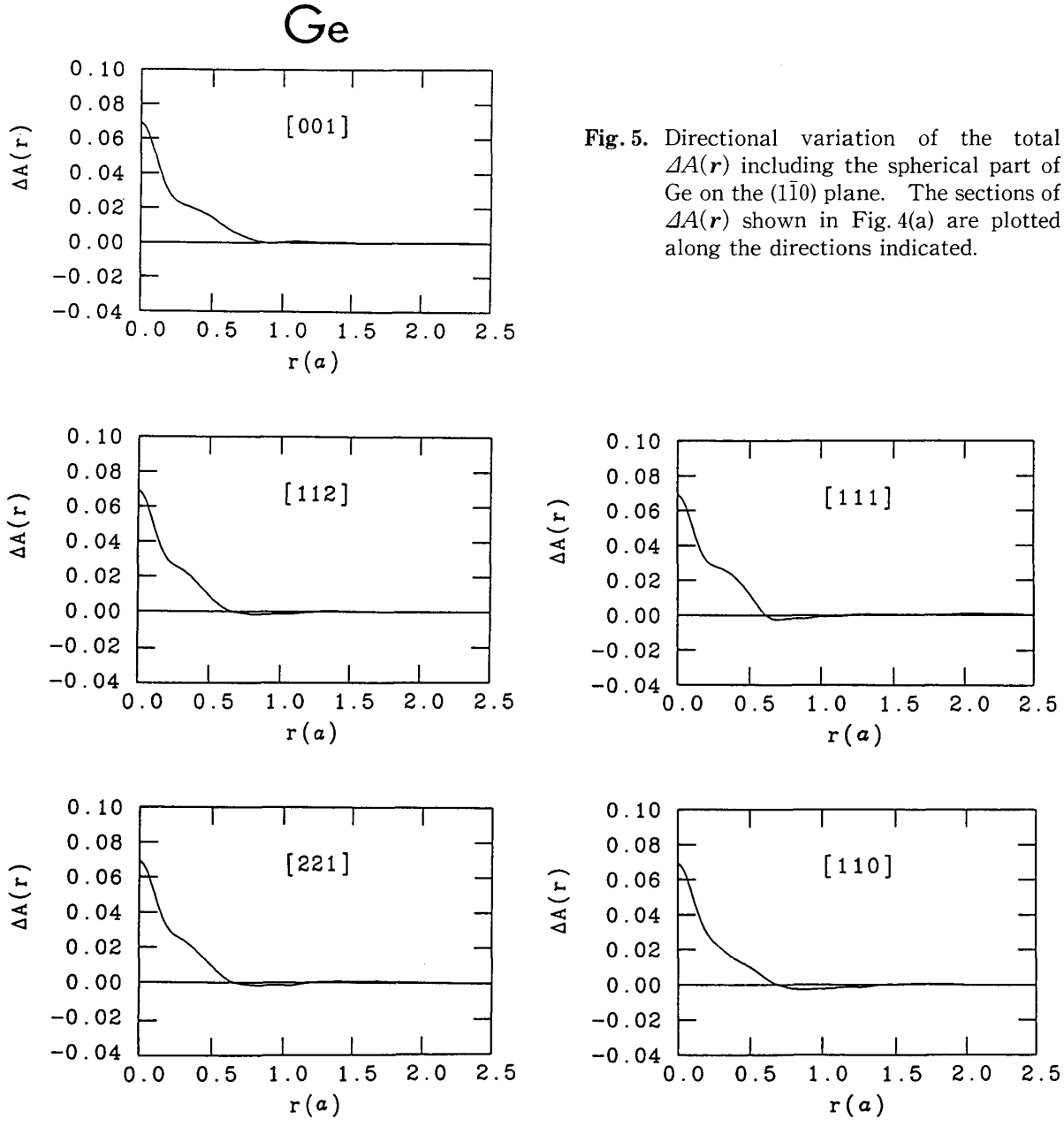

Fig. 5. Directional variation of the total $\Delta A(\boldsymbol{r})$ including the spherical part of Ge on the $(1\bar{1}0)$ plane. The sections of $\Delta A(\boldsymbol{r})$ shown in Fig. 4(a) are plotted along the directions indicated.

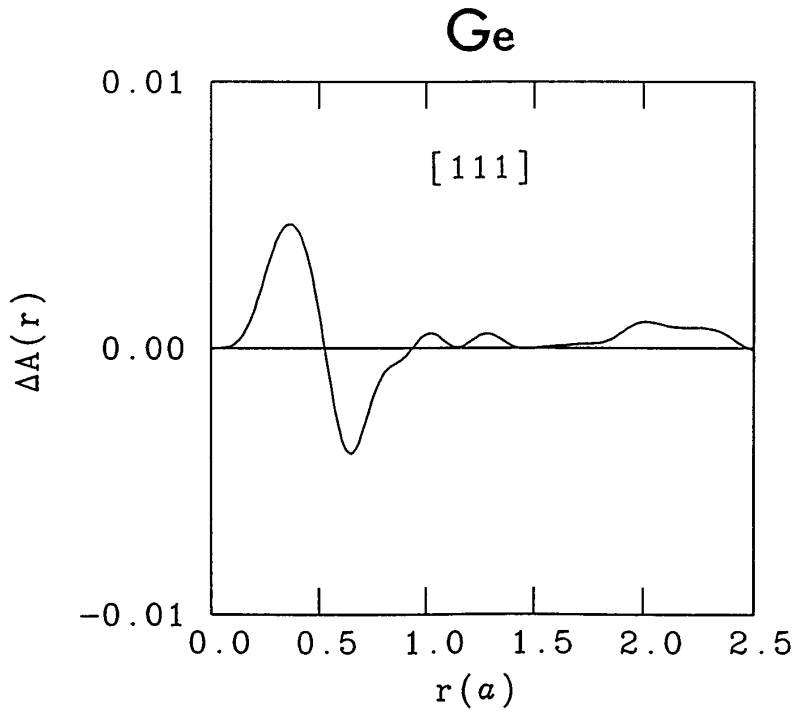

Fig. 6. Directional variation of the anisotropic part of $\Delta A(\boldsymbol{r})$ of Ge along the [111] direction.

2). On the other hand, being attracted by the valence electrons, the positron makes also a lower density peak around the valence bonding centre (Fig. 4 in ref. 2). The weak pair distribution in the valence bond region may be a prime cause of the local pattern.

Since the positron feels the electron CO terms indirectly through the Coulomb interaction with valence electrons[3] and, as mentioned above, the positron distribution is not dense in the main distribution region of valence electrons, we can expect that the CO effect on the $A(\boldsymbol{r})$-function may be fairly small. In Fig. 4, (a) shows the contour map of the total $\Delta A(\boldsymbol{r})$ and (b) its anisotropic behaviour, where the types of contour lines are the same in Figs. 1 and 2, and the contour spacings are 0.005 and 0.001, respectively. In order to visualize the weak CO contribution, such a narrow contour spacings are necessary. Directional variations along the five directions are given in Fig. 5 for the total $\Delta A(\boldsymbol{r})$. The total $\Delta A(\boldsymbol{r})$ damps sharply with much weaker anisotropic shoulder. The shoulder structure is due to a new local pattern with closed contour lines observed in the anisotropic $\Delta A(\boldsymbol{r})$ around the point of $r=0.36a$ in the [111] direction, which is arrowed in Fig. 4(b). Again, the point differs from the nearest neighbour atom site at $r=0.4330a$ or the bonding centre at $r=0.2165a$. Figure 6 shows the directional variation of the anisotropic $\Delta A(\boldsymbol{r})$ along the [111] direction in the enlarged scale. The peak structure of the closed local pattern corresponds to that observed clearly in the anisotropic part of the Compton $\Delta B(\boldsymbol{r})$ [see Fig. 7(b) in ref. 8], while the peak value of the latter is much larger than that of the former and the centre of the peak is just located on the nearest neighbour atom site. The former has been analyzed[8] as an image pattern reflecting well the atomic and crystallographic structures of the nearest neighbour

atom, by using the fact that the $B(\boldsymbol{r})$-function is described in terms of the autocorrelation function between the electron wave functions[15]. The closed local pattern in the $\Delta A(\boldsymbol{r})$-function is shifted from the nearest neighbour atom in position and size.

As was shown in ref. 19, the $A(\boldsymbol{r})$-function can be related to the autocorrelation function between the electron-positron pair wave functions as

$$A(\boldsymbol{r})=2\sum_{n}\sum_{k}\int\Phi_{nk}^{*}(\boldsymbol{r}')\Phi_{nk}(\boldsymbol{r}'+\boldsymbol{r})d^{3}\boldsymbol{r}', \quad (5)$$

where

$$\Phi_{nk}(\boldsymbol{r})=\Psi_{nk}(\boldsymbol{r})\Psi_{+}(\boldsymbol{r}). \quad (6)$$

By analogy with the discussion[8] for the $\Delta B(\boldsymbol{r})$-function, we can connect the local pattern in the $\Delta A(\boldsymbol{r})$-function with a kind of image of the nearest neighbour atom. However, the image cannot reproduce the structural information of the atom directly. Through the CO mechanism coupled with the characteristic distribution of positron, we obtain an atom-like pattern fairly modified in position and size of the atom. The weakness of the pattern is consistent with the relatively weak piling up of positron in the region of valence bond.

Theoretically, the problem is interesting for discussing appropriateness among various theoretical approaches to quantitatively fine calculation of electronic and positronic states. At the present stage of resolution power in experiments, however, it may be very difficult to detect the weak pattern clearly.

References

1) Kobayasi, T. and Nara, H.: The Valence Electronic Charge Densities of Si and Ge and the Effect of Core-Orthogonalization, Bull. Coll. Med. Sci. Tohoku Univ., **1**, 15-26, 1992
2) Kobayasi, T. and Nara, H.: Core-Orthogonalization Effect in Pseudopotential Theory of the Charge Density Distribution of Valence Electrons in Semiconductors with Comments on the Effects in Momentum Space, Z. Naturforsch., **48a**, 193-197, 1992
3) Kobayasi, T.: Fourier Inversion Formalism for the Calculation of Angular Correlation of Positron Annihilation Radiation of Semiconductors, Bull. Coll. Med. Sci. Tohoku Univ., **3**(1), 11-22, 1994
4) Kobayasi, T.: Core-Orthogonalization Effect on the Momentum Density Distribution of Valence Electron-Positron Pairs in Semiconductors, Bull. Coll. Med. Sci. Tohoku Univ., **4**(1), 17-28, 1995
5) Kobayasi, T. and Nara, H.: Improvement of Theoretical ACAR of Semiconductors including High Momentum Region, Positron Annihilation (Material Science Forum Vols. **175-178**, Part 2), ed. by He, Y.-J., Cao, B.-S. and Jean, Y.C., Trans Tech Pub., Aedermannsdorf, 1995, pp. 903-908
6) Kobayasi, T., Nara, H., Timms, D.N. and Cooper, M.J.: Core-Orthogonalization Effects on the Momentum Density Distribution and the Compton Profile of Valence Electrons in Semiconductors, Bull. Coll. Med. Sci. Tohoku Univ., **4**(2), 93-104, 1995
7) Kobayasi, T.: Core-Orthogonalization Effect on the Compton Profiles of Valence Electrons in Si, Bull. Coll. Med. Sci. Tohoku Univ., **5**(2), 149-164, 1996
8) Kobayasi, T.: Image of Intra-Unit-Cell Atom Appearing in Compton $B(\boldsymbol{r})$-Function: "Compton Microscope"?, Bull. Coll. Med. Sci. Tohoku Univ., **6**(1), 11-22, 1997
9) Pattison, P. and Williams, B.: Fermi Surface Parameters from Fourier Analysis of Compton Profiles, Solid State Commun., **20**, 585-588, 1976
10) Mueller, F.M.: Anisotropic Momentum Densities from Compton Profiles: Silicon, Phys. Rev., **B15**, 3039-3044, 1977
11) Shülke, W.: The One-Dimensional Fourier Transform of Compton Profiles, Phys. Stat. Sol. (b), **82**, 229-235, 1977

12) Kramer, B., Krusius, P., Schröder, W. and Schülke, W.: Fourier-Transformed Compton Profiles: A Sensitive Probe for the Microstructure of Semiconductors, Phys. Rev. Lett., **38**, 1227-1230, 1977
13) Mijnarends, P.E.: Reconstruction of Three-Dimensional Distribution, Compton Scattering, ed. by Williams, B., MacGraw-Hill, New York, 1977, pp. 323-345
14) Nara, H., Shindo, K. and Kobayasi, T.: Pseudopotential Approach to Anisotropies of Compton-Profiles of Si and Ge, J. Phys. Soc. Jpn., **46**, 77-83, 1979
15) Cooper, M.J.: Compton Scattering and Electron Momentum Determination, Rep. Prog. Phys., **48**, 415-481, 1985
16) Nara, H. and Kobayasi, T.: Nonlocal Pseudopotentials of Si and Ge, J. Phys. Soc. Jpn., **41**, 1429-1430, 1976
17) Kobayasi, T. and Nara, H.: Properties of Nonlocal Pseudopotentials of Si and Ge Optimized under Full Interdependence among Potential Parameters, Bull. Coll. Med. Sci. Tohoku Univ., **2**(1), 7-16, 1993
18) Mueller, F.M. and Priestley, M.G.: Inversion of Cubic de Haas-van Alphen Data, with an Application to Palladium, Phys. Rev., **148**, 638-643, 1966
19) Kobayasi, T.: Coupling of Positron Annihilation and Compton Scattering : A Proposal of a Positron Autocorrelation Function with Reduction of the Effect of Electron Distribution, Bull. Coll. Med. Sci. Tohoku Univ., **5**(1), 87-90, 1996